Front. Phys. 10, 100507 (2015)
DOI 10.1007/s11467-015-0501-1

RESEARCH ARTICLE

Quadrupolar matter-wave soliton in two-dimensional free space

Jia-Sheng Huang[1], Xun-Da Jiang[1], Huai-Yu Chen[1], Zhi-Wei Fan[1], Wei Pang[2], Yong-Yao Li[1,†]

[1] *Department of Applied Physics, College of Electronic Engineering, South China Agricultural University, Guangzhou 510642, China*

[2] *Department of Experiment Teaching, Guangdong University of Technology, Guangzhou 510006, China*

Corresponding author. E-mail: †yongyaoli@gmail.com

Received May 14, 2015; accepted June 23, 2015

We study two-dimensional (2D) matter-wave solitons in the mean-field models formed by electric quadrupole particles with long-range quadrupole–quadrupole interaction (QQI) in 2D free space. The existence of 2D matter-wave solitons in the free space was predicted using the 2D Gross–Pitaevskii Equation (GPE). We find that the QQI solitons have a higher mass (smaller size and higher intensity) and stronger anisotropy than the dipole–dipole interaction (DDI) solitons under the same environmental parameters. Anisotropic soliton–soliton interaction between two identical QQI solitons in 2D free space is studied. Moreover, stable anisotropic dipole solitons are observed, to our knowledge, for the first time in 2D free space under anisotropic nonlocal cubic nonlinearity.

Keywords 2D matter-wave solitons, quadrupole–quadrupole interaction, anisotropy soliton–soliton interaction, dipole solitons

PACS numbers 05.45.Yv, 03.75.Lm, 43.25.Rq, 94.05.Fg

1 Introduction

The Bose–Einstein condensate (BEC), which is a macroscopic quantum state of matter, was theoretically predicted by Bose and Einstein 90 years ago [1]. In the past few decades, scientists have performed much theoretical and experimental research in the field of BECs after a BEC was first observed in dilute alkali gases. Rich phenomena have been revealed in the studies of BEC, such as solitons [2, 3], vortex formation [4, 5], Josephson oscillation [6, 7], chaos [8], and symmetry breaking [9–12]. The matter-wave soliton was also experimentally observed in ultra-cold atom gases [13, 14], and with the development of Feshbach resonance [15–17], it plays a crucial role in the research on solitons [18–21].

As is well known, stable two-dimensional (2D) matter-wave solitons are more significant than one-dimensional (1D) solitons in terms of both theoretical interest and potential for applications, which makes them crucial in the study of matter-wave solitons. It is also well known that cubic nonlinearity is the most common type of nonlinearity in nature, and the modulation instability in such nonlinearity leads to the collapse of solitons in 2D free space [22]. There are two methods to overcome this instability and obtain a stable 2D soliton in the cubic nonlinear material. The first involves the introduction of a periodical potential through structures such as 2D waveguide arrays or optical lattices [23, 24]. The periodical potential introduces new features, such as lattice solitons [26–28], lattice gap solitons [29], and lattice vortex solitons [30, 24, 31]. However, it also breaks the translation symmetry and rotational symmetry of the system, limiting the mobility of the solitons. The other method involves introducing long-range interactions. For example, isotropic long-range Van der Waals interactions between Rydberg atoms in ultra-cold boson gases [33, 34], anisotropic long-range dipole–dipole interactions (DDI) in dipolar condensates [35–40], etc. Introducing long-range interaction can not only stabilize 2D matter-wave solitons but also enhance the mobility and soliton–soliton interactions for solitons in free space.

Recently, we studied matter-wave solitons supported by anisotropic long-range quadrupole–quadrupole interaction (QQI) inter-site interactions in quadrupolar condensates [43]. In that work, we built stable 2D matter-wave solitons maintained by long-range QQI in a deep 2D optical lattice. However, realizing stable solitons with QQI in 2D free space is more challenging. In the present study, we propose a model to produce stable solitons in 2D free space and systematically study their interactions. Moreover, under the actions of QQI, stable 2D dipole

solitons are observed. To our knowledge, in the background of anisotropic nonlocal nonlinearity, such solitons have not been reported in the literature.

The objective of this work is to study the shapes and interactions of 2D matter-wave solitons in BECs formed by quadrupole particles in 2D free space. The model describing this system is derived in Section 2. Numerical results of fundamental solitons and their interactions as well as dipolar solitons and their properties are systematically studied in Section 3. The paper is concluded in Section 4.

2 The model

2.1 The system induced by QQI

Two types of quadrupoles exist: electric quadrupoles and magnetic quadrupoles. Because magnetic quadrupolar BECs have been proved unsuitable to support 2D bright solitons in free space [43], we only consider electric quadrupolar BECs in this work. The electric quadrupoles are built as tightly bound pairs of dipoles and anti-dipoles, which are directed perpendicular to the systems' plane (x, y), i.e., along the z axis. Its strength is a linearly growing function of x. Such an external electric field can be stimulated by a tapered capacitor, as shown in Fig. 1. These electric quadrupoles can be described by a symmetric traceless tensor $Q_{\alpha\beta}$ $(\alpha, \beta = x, y, z)$ with $\Sigma_\alpha Q_{\alpha\alpha} \equiv 0$ [44]; therefore, in the setting of Fig. 1, they have the following components in this notation:

$$Q_{xy} = Q_{yx} \equiv Q; Q_{zz} = Q_{zx} = Q_{xz} = Q_{yz} = 0, \tag{1}$$

where the quadrupole moment is defined as

$$Q = 3d\varepsilon, \tag{2}$$

$\pm d$ are the dipolar moments of the bound dipoles and anti-dipoles, and ε is the distance between them.

Between two quadrupoles in the planar configuration considered here, the potential of the interaction can be derived from the general formula for the QQI potential as

$$U_{QQ}^{(electr)}(r, \theta) = \frac{4}{3} Q^2 r^{-5} (1 - 5\cos^2\theta), \tag{3}$$

where r is the distance between the quadrupoles while θ is the angle between the vector connecting the quadrupoles and the line connecting the dipole and anti-dipole inside the quadrupole.

The mean-field dynamics of solitons in this setting is described by the underlying 2D Gross–Pitaevskii Equation (GPE) [42]:

$$\mathrm{i}\frac{\partial \psi}{\partial t} = -\frac{1}{2}\left(\frac{\partial^2}{\partial x^2} + \frac{\partial^2}{\partial y^2}\right)\psi + g|\psi|^2\psi + \kappa\psi(\boldsymbol{r}) \int \mathrm{d}\boldsymbol{r}' K(\boldsymbol{r} - \boldsymbol{r}')|\psi(\boldsymbol{r}')|^2, \tag{4}$$

where $\boldsymbol{r} \equiv \{x, y\}$ is the position of the quadrupole, g is the local nonlinear parameter of the system ($g < 0$ indicates contact self-attraction while $g > 0$ indicates contact self-repulsion), and κ is the strength of nonlocal nonlinearity. In this work, κ is fixed as $\kappa \equiv 1$. The kernel in the integral term, which provides the QQI interaction between the particles, is defined as

$$K_{QQ}(\boldsymbol{r} - \boldsymbol{r}') = \frac{1 - 5\cos^2\theta}{[b^2 + (\boldsymbol{r} - \boldsymbol{r}')^2]^{5/2}}, \tag{5}$$

where b, which is fixed to 0.2 in the following discussion, is the regularization scale provided by the thickness of the confined layer in the z direction. If we replace this kernel by

$$K_{DD}(\boldsymbol{r} - \boldsymbol{r}') = \frac{1 - 3\cos^2\theta}{[b^2 + (\boldsymbol{r} - \boldsymbol{r}')^2]^{3/2}}, \tag{6}$$

Equation (4) can be applied to describe the mean-field dynamics of 2D dipolar matter-wave solitons [38, 39].

We assume the solitons have the form

$$\psi(\boldsymbol{r}, t) = \phi(\boldsymbol{r})\mathrm{e}^{-\mathrm{i}\mu t}, \tag{7}$$

where $\phi(\boldsymbol{r})$ is the stationary form of the soliton solution and μ is its chemical potential. The total norm is defined by

$$N = \int |\phi(\boldsymbol{r})|^2 \mathrm{d}\boldsymbol{r}. \tag{8}$$

In the following sections, the solitons are numerically studied. For the stationary solution, the numerical method we use is imaginary-time propagation (ITP) [47–49], while for the dynamical real-time evolution, the numerical method we use is the split-step Fourier transformation [50]. In order to study the formation of solitons solely from the anisotropic nonlocal nonlinearity, we fix the local nonlinear parameter $g \equiv 0$ in this paper. This

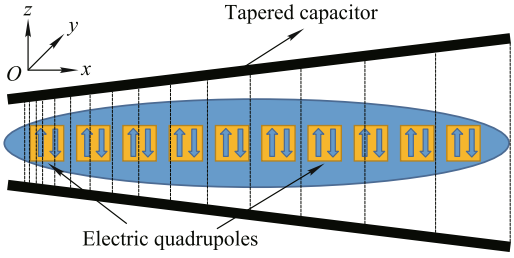

Fig. 1 Electric quadrupole was built as tightly bound pairs of dipole and anti-dipole, which are directed perpendicular to the systems' plane (x, y), i.e., along axis z. The strength of the quadrupole is a linearly growing function of x.

treatment can be physically achieved via Feshbach resonance [15–17].

3 Numerical results

3.1 Anisotropic fundamental soliton

Figure 2 shows typical examples of stable fundamental matter-wave solitons maintained by QQI and DDI based on Eq. (4) with kernels (5) and (6), respectively. Their total norm is $N = 1.5$. This figure shows that the QQI solitons feature stronger anisotropy and their occupied area is far smaller than that of the DDI solitons, which makes their intensity higher than that of the DDI solitons.

To quantify the solitons between the DDI and QQI further, we define their effective area $A_{\rm eff}$ and structural anisotropy η between the horizontal ("$A_{\rm effx}$") and vertical ("$A_{\rm effy}$") directions as follows:

$$A_{\rm eff} = \frac{\left(\iint |\psi|^2 {\rm d}x{\rm d}y\right)^2}{\iint |\psi|^4 {\rm d}x{\rm d}y}, \tag{9}$$

$$\eta = \frac{|A_{\rm effx} - A_{\rm effy}|}{A_{\rm effx} + A_{\rm effy}}, \tag{10}$$

where

$$A_{\rm effx} = \frac{\left[\int |\psi(x,0)|^2 {\rm d}x\right]^2}{\int |\psi(x,0)|^4 {\rm d}x},$$

$$A_{\rm effy} = \frac{\left[\int |\psi(0,y)|^2 {\rm d}y\right]^2}{\int |\psi(0,y)|^4 {\rm d}y}. \tag{11}$$

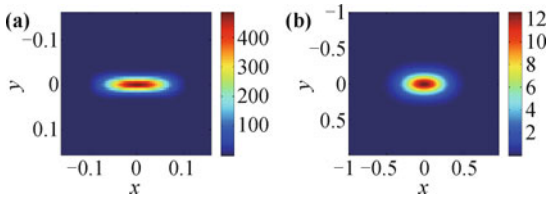

Fig. 2 Stable fundamental solution for matter-wave soliton maintained by QQI **(a)** and DDI **(b)**. The total norm are all equal to 1.5.

Figure 3 shows a comparison of these two characters [Eqs. (9) and (10)] as well as μ versus N for two types of solitons. In Figs. 3(a) and (b), the area and degree of anisotropy (i.e., $A_{\rm eff}$ and η) of both types of solitons decreases and increases, respectively, with increasing N; however, the area of the QQI solitons is two orders smaller than that of the DDI solitons for the same magnitude of N, and the degree of anisotropy of the QQI solitons is approximately twice that of the DDI solitons for the same N. In Fig. 3(c), both solitons satisfy ${\rm d}\mu/{\rm d}N < 0$, i.e., the Vakhitov–Kolokolov criterion, which is a well-known necessary stable condition for modes supported by attractive nonlinearities [45, 46]. For the magnitude of μ, the QQI solitons are more than two orders smaller than the DDI solitons for the same N.

These phenomena can be explained by the difference between the two kernels in Eqs. (5) and (6). The denominators of these two kernels are $\sim 1/r^5$ and $\sim 1/r^3$, respectively. Therefore, QQI features more compactly nonlocal effect than DDI, causing the QQI solitons to be heavier (smaller size and higher intensity) than the DDI solitons. Moreover, in the numerators of both kernels, the coefficient before $\cos^2\theta$ for QQI is 5, while that for DDI is 3, causing the QQI solitons to have an anisotropy that is approximately twice that of the DDI solitons. Furthermore, the threshold for forming a soliton in the QQI case is smaller than that in the DDI case, and the QQI case has a wider stability area than the DDI case.

3.2 Anisotropic soliton–soliton interaction

In this subsection, we study for the anisotropic interaction between the QQI solitons through the real-time evolution of Eq. (4) from an initial condition, which is constructed by two identical solitons placed at a pair of zero-point symmetric positions defined by

$$\psi(\boldsymbol{r}, t=0) = \phi(x+x_0, y+y_0) + \phi(x-x_0, y-y_0). \tag{12}$$

According to kernel (5), when the angle θ satisfies

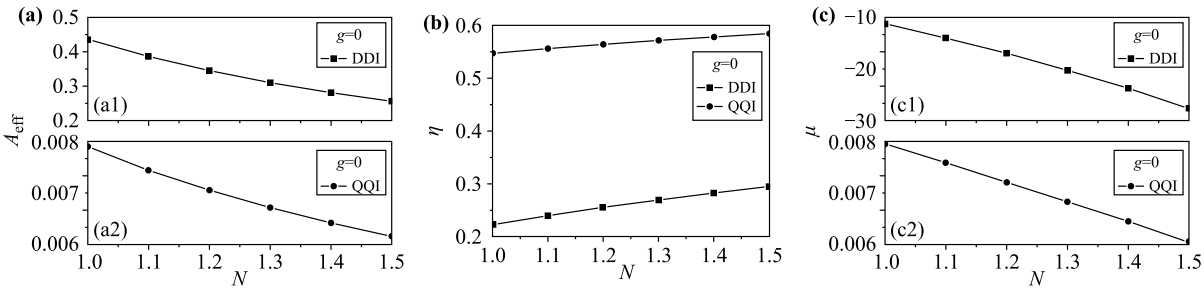

Fig. 3 **(a)** Effective area $A_{\rm eff}$ [see Eq. (9)] versus the norm for the solitons supported by the DDI (a1) and QQI (a2). **(b)** The anisotropy η [see Eq. (10)] versus N for two types of solitons. **(c)** The chemical potential μ for two types of soliton versus N.

$1 - 5\cos^2\theta = 0$ (i.e., $\theta \approx 63.44°$ or $116.56°$), the QQI is zero; therefore, these two typical angles form the borders between the repulsive and attractive QQI. Figure 4 shows the interaction map of the zero-symmetric soliton pair starting from (12) in the x_0–y_0 plane. Because the QQI interaction is a long-range interaction, the two solitons automatically interact with each other when placed inside the plane. Generally, there are two types of interactions between the solitons: attraction and repulsion. The soliton will set into mobility through these two types of interactions without any kicks acting on them. As shown in Fig. 4, if the center of the solitons were initially placed in the yellow areas, the interaction between them is attractive; the two solitons move toward each other and eventually merge into a single one. Typical examples of such dynamics are displayed in Figs. 5(a1)–(a3). In contrast, in the blue areas, the two solitons are repelled away from each other because of repulsive interaction; typical examples of such dynamics are displayed in Figs. 5(b1)–(b3). If the center of the solitons is initially placed in the white (blank) area, the soliton pair shows no obvious interaction within $t = 100 \times A_{\mathrm{effx}}^2$, which implies that the distance between them is sufficiently high for the interactions between them to be negligible.

The red dashed lines in Fig. 4 are the theoretical boundaries of attractive and repulsive interaction, along which the interaction of QQI is equal to zero. As predicted by kernel (5), the borders between blue and yellow areas approximately coincide with the red dashed lines. An interesting phenomenon is that the soliton pair features attraction in the area of $63.44° < \theta < 116.56°$ when $-0.094 < y_0 < 0.094$. Typical examples of such

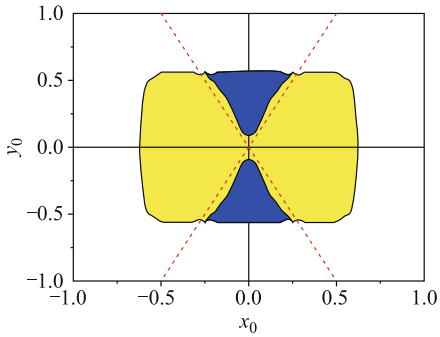

Fig. 4 The distribution of soliton-soliton interaction in the x_0–y_0 plane maintained by QQI. When the two identical solitons placed with zero-symmetry inside the blue colored areas, they repel each other. However, when these two solitons placed with zero-symmetry inside the yellow colored areas, they attract each other. In the white colored area two solitons do not show obvious interaction tendency within the time of 100 times the diffraction length (i.e., $100 \times A_{\mathrm{effx}}^2$). The red dashed lines are the theoretical boundary of attractive and repulsive interaction, which are obtained from $1 - 5\cos^2\theta = 0$. Along the lines, the QQI is zero. Here, the norm of two solitons is fixed as 1.5, and the coefficient of the local nonlinearity is fixed by $g = 0$.

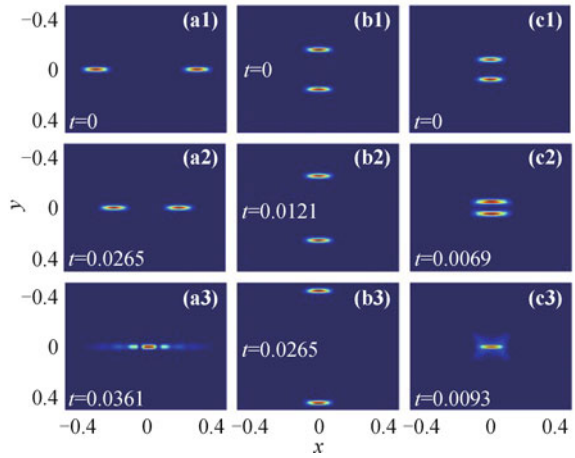

Fig. 5 Typical example for soliton-soliton interaction supported by QQI. The total norm of the identical solitons is per 1.5. **(a1–a3)** Typical example for dynamics of the attractive interaction between soliton pair along the horizontal direction, where the two identical solitons are initially placed at $(x_0, y_0) = (\pm 0.31, 0)$, respectively. **(b1–b3)** Typical example for dynamics of the repulsive interaction between soliton pair along the vertical direction, where the two identical solitons are initially placed at $(x_0, y_0) = (0, \pm 0.16)$, respectively. **(c1–c3)** Typical example for the dynamic of attractive interaction between the soliton pair along the vertical direction, where the two identical solitons are initially placed at $(x_0, y_0) = (0, \pm 0.08)$, respectively.

dynamics are displayed in Figs. 5(c1)–(c3). In this case, the attraction results from the thin and long profile of the soliton along the horizontal direction. When the two solitons are placed sufficiently close (i.e., $|y_0| < 0.094$), such attraction overcomes the repulsion. However, this attraction decays more quickly than the repulsion when the distance between the soliton pair is increased, causing the soliton pair to have repulsive interaction after $|y_0| > 0.094$. Another interesting phenomenon is that the soliton pair rotates before merging or bouncing away, when the solitons are launched close to the two dashed lines. Because the solitons have a finite size, some part of the soliton crosses the border and extends to the other side, resulting in the combined action of repulsion and attraction between the soliton pair. Such combined action creates a torque between the solitons, resulting in the rotational motion between them. Figures 6 and 7 show typical examples of such dynamics. In Fig. 6, two solitons are rotating with mutual attraction when the center of the solitons is arranged diagonally in the yellow region close to the dashed line. In Fig. 7, two solitons are rotating with mutually repulsion when the center of the solitons is arranged diagonally in the blue region close to the dashed line.

3.3 Anisotropic dipole soliton

Dipole matter-wave solitons are also observed in this

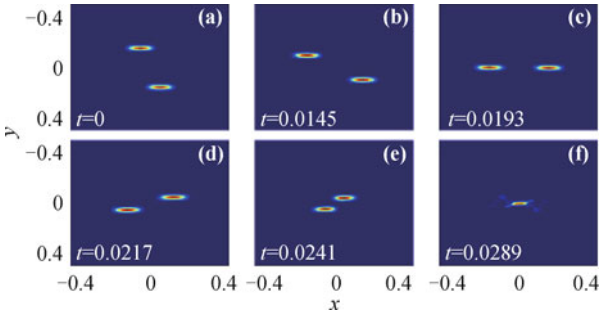

Fig. 6 The dynamical evolution with a mutual attraction. Here we select $(x_0, y_0) = (0.063, 0.156)$ in Eq. (12) and the total norm of the soliton is per 1.5.

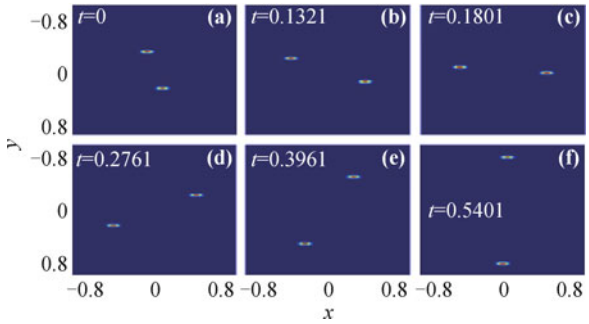

Fig. 7 The dynamical evolution with a mutual repulsion. Here we select $(x_0, y_0) = (0.094, 0.281)$ in Eq. (12) and the total norm of the soliton is per 1.5.

model. It is found that the dipole soliton is stable when $N > 0.18$. A typical example of such solitons is displayed in Fig. 8. Figure 8(d1) demonstrates that the width of this type of solitons decreases with increasing N. Figure 8(d2) shows that the μ–N relation of this kind of solitons satisfies $\mathrm{d}\mu/\mathrm{d}N < 0$, the Vakhitov–Kolokolov criterion.

When $N < 0.18$, the dipole soliton decays to a moving fundamental soliton. A typical example of this process is shown in Fig. 9. In this process, the intensity distribution of the soliton becomes asymmetric with one part absorbing into another part [See Figs. 9(a) and (b)], and then it finally becomes a moving fundamental soliton [See Fig. 9(c)]. This phenomenon can be explained as follows: unlike the fundamental solitons, dipole solitons are in an excited state, and their formation requires stronger nonlinearity. If the nonlinearity is not sufficient, the dipole

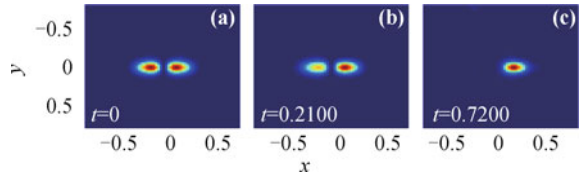

Fig. 9 Typical examples of real-time evolution for unstable dipole solution for matter-wave soliton for $N = 0.14$.

soliton decays to a fundamental one, which does not require as much nonlinearity [51]. To our knowledge, in 2D free space, this is the first observation of such solitons under anisotropic nonlocal cubic nonlinearity.

4 Conclusion

We studied two-dimensional matter-wave solitons formed by electric quadrupole particles in mean-field models with long-range quadrupole–quadrupole interaction between particles in 2D free space. The quadrupoles have two straightforward settings: electric quadrupole and magnetic quadrupole. This work was based on electric quadrupolar particles. We applied the 2D Gross–Pitaevskii Equation with the long-range QQI term under the mean-field approximation to describe the dynamics of the solitons. Shapes, stability, and anisotropy of the fundamental and dipolar matter-wave solitons were investigated in 2D free space. The anisotropic soliton–soliton interaction between the fundamental solitons was systematically studied, and the distribution map of soliton–soliton interaction was plotted. Through a comparison between the QQI and DDI cases, we found that the QQI solitons have a higher mass (smaller size and higher intensity) and stronger anisotropy than the DDI solitons under the same environmental parameters. Moreover, a stable anisotropic dipole soliton is observed for the first time in 2D free space under anisotropic nonlocal cubic nonlinearity.

Acknowledgements This work was supported by the National Natural Science Foundation of China (Grant Nos. 11104083, 11204089, and 11205063). Authors appreciate the very useful discussion from Prof. Boris A. Malomed.

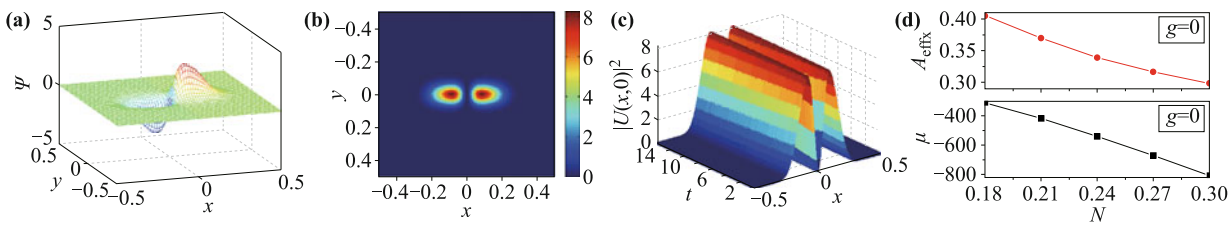

Fig. 8 Stable matter-wave soliton maintained by QQI for $N = 0.2$. **(a)** Amplitude of the soliton. **(b)** Intensity distribution of the soliton. **(c)** Real-time evolution with 1% initial random perturbation, which proves this soliton is stable. **(d)** Horizontal length [cf. Eq. (11)] of the soliton and the chemical potential of the soliton versus N, respectively.

References

1. L. P. Pitaevskii and S. Sandro, Bose–Einstein Condensation, No. 116, Oxford University Press, 2003
2. S. Burger, K. Bongs, S. Dettmer, W. Ertmer, and K. Sengstock, Dark solitons in Bose-Einstein condensates, *Phys. Rev. Lett.* 83(25), 5198 (1999)
3. S. Song, L. Wen, C. Liu, S. Gou, and W. Liu, Ground states, solitons and spin textures in spin-1 Bose–Einstein condensates, *Front. Phys.* 8(3), 302 (2013)
4. B. P. Anderson, P. C. Haljan, C. A. Regal, D. L. Feder, L. A. Collins, C. W. Clark, and E. A. Cornell, Watching dark solitons decay into vortex rings in a Bose–Einstein condensate, *Phys. Rev. Lett.* 86(14), 2926 (2001)
5. J. R. Abo-Shaeer, C. Raman, J. M. Vogels, and W. Ketterle, Observation of vortex lattices in Bose–Einstein condensates, *Science* 292(5516), 476 (2001)
6. F. S. Cataliotti, S. Burger, C. Fort, P. Maddaloni, F. Minardi, A. Trombettoni, A. Smerzi, and M. Inguscio, Josephson junction arrays with Bose-Einstein condensates, *Science* 293(5531), 843 (2001)
7. C. Lee, W. Hai, L. Shi, X. Zhu, and K. Gao, Chaotic and frequency-locked atomic population oscillations between two coupled Bose-Einstein condensates, *Phys. Rev. A* 64(5), 053604 (2001)
8. C. Lee, J. Huang, H. Deng, H. Dai, and J. Xu, Nonlinear quantum interferometry with Bose condensed atoms, *Front. Phys.* 7(1), 109 (2012)
9. C. Lee, Universality and anomalous mean-field breakdown of symmetry-breaking transitions in a coupled two-component Bose–Einstein condensate, *Phys. Rev. Lett.* 102(7), 070401 (2009)
10. H. Zheng and Q. Gu, Dynamics of Bose–Einstein condensates in a one-dimensional optical lattice with double-well potential, *Front. Phys.* 8(4), 375 (2013)
11. Y. Li, J. Liu, W. Pang, and B. A. Malomed, Symmetry breaking in dipolar matter-wave solitons in dual-core couplers, *Phys. Rev. A* 87(1), 013604 (2013)
12. Y. Li, W. Pang, and B. A. Malomed, Nonlinear modes and symmetry breaking in rotating double-well potentials, *Phys. Rev. A* 86(2), 023832 (2012)
13. J. Denschlag, Generating solitons by phase engineering of a Bose–Einstein condensate, *Science* 287, 97 (2000)
14. Khaykovich, F. Schreck, G. Ferrari, T. Bourdel, J. Cubizolles, L. D. Carr, Y. Castin, and C. Salomon, Formation of a matter-wave bright soliton, *Science* 296, 1290 (2002)
15. Ph. Courteille, R. S. Freeland, D. J. Heinzen, F. A. van Abeelen, and B. J. Verhaar, Observation of a Feshbach resonance in cold atom scattering, *Phys. Rev. Lett.* 81, 69 (1998)
16. M. Theis, G. Thalhammer, K. Winkler, M. Hellwig, G. Ruff, R. Grimm, and J. Hecker Denschlag, Tuning the scattering length with an optically induced Feshbach resonance, *Phys. Rev. Lett.* 93(1), 123001 (2004)
17. X. Zhang, X. Hu, D. Wang, X. Liu, and W. Liu, Dynamics of Bose-Einstein condensates near Feshbach resonance in external potential, *Front. Phys. China* 6(1), 46 (2011)
18. S. Inouye, M. R. Andrews, J. Stenger, H.-J. Miesner, D. M. Stamper-Kurn and W. Ketterle, Observation of Feshbach resonances in a Bose–Einstein condensate, *Nature* 293(6672), 151 (1998)
19. P. Courteille, R. S. Freeland, D. J. He inzen, F. A. van Abeelen and B. J. Verhaar, Observation of Feshbach resonances in cold atom scattering, *Phys. Rev. Lett.* 81, 69 (1998)
20. J. Huang, H. Li, X. Zhang, and Y. Li, Transmission, reflection, scattering, and trapping of traveling discrete solitons by $\mathcal{C}$ and $\mathcal{V}$ point defects, *Front. Phys.* 10(2), 104201 (2015)
21. Z. Chen, J. Huang, J. Chai, X. Zhang, Y. Li, and B. A. Malomed, Discrete solitons in self-defocusing systems with PT -symmetric defects, *Phys. Rev. A* 91(5), 053821 (2015)
22. M. Saha, A. K. Sarma, Modulation instability in nonlinear metamaterials induced by cubic–quintic nonlinearities and higher order dispersive effects, *Opt. Commun.* 291, 321 (2013)
23. J. W. Fleischer, M. Segev, N. K. Efremidis, and D. N. Christodoulides, Observation of two-dimensional discrete solitons in optically induced nonlinear photonic lattices, *Nature* 422(6928), 147 (2003)
24. G. Chen, Z. Hong, and Z. Mai, Two-dimensional discrete Anderson location in waveguide matrix, *J. Nonlinear Optic. Phys. Mat.* 23(03), 1450033 (2014)
25. X. Zhang, J. Chai, D. Ou, and Y. Li, Antisymmetry breaking of discrete dipole gap solitons induced by a phase-slip defect, *Mod. Phys. Lett. B* 28(12), 1450097 (2014)
26. N. K. Efremidis and D. N. Christodoulides, Lattice solitons in Bose–Einstein condensates, *Phys. Rev. A* 67(6), 063608 (2003).
27. N. K. Efremidis, J. Hudock, D. N. Christodoulides, J. W. Fleischer, O. Cohen, and M. Segev, Two-dimensional optical lattice solitons, *Phys. Rev. Lett.* 91(21), 213906 (2003)
28. W. Pang, J. Wu, Z. Yuan, Y. Liu, and G. Chen, Lattice solitons in optical lattice controlled by electromagnetically induced transparency, *J. Phys. Soc. Jpn.* 80(11), 113401 (2011)
29. J. T. Cole and Z. H. Musslimani, Band gaps and lattice solitons for the higher-order nonlinear Schrödinger equation with a periodic potential, *Phys. Rev. A* 90(1), 013815 (2014)
30. X. Gan, P. Zhang, S. Liu, F. Xiao, and J. Zhao, Beam steering and topological transformations driven by interactions between a discrete vortex soliton and a discrete fundamental soliton, *Phys. Rev. A* 89(1), 013844 (2014)
31. G. Chen, H. Huang, and M. Wu, Solitary vortices in two-dimensional waveguide matrix, *J. Nonlinear Optic. Phys. Mat.* 24(01), 1550012 (2015)
32. G. Chen, H. Huang, and M. Wu, Discrete vortices on anisotropic lattices, *Front. Phys.* 10, 104206 (2015)

33. R. Heidemann, U. Raitzsch, V. Bendkowsky, B. Butscher, R. Low, and T. Pfau, Rydberg excitation of Bose–Einstein condensates, *Phys. Rev. Lett.* 100(3), 033601 (2008)
34. M. Viteau, M. G. Bason, J. Radogostowicz, N. Malossi, D. Ciampini, O. Morsch, and E. Arimondo, Rydberg excitations in Bose–Einstein condensates in quasi-one-dimensional potentials and optical lattices, *Phys. Rev. Lett.* 107(6), 060402 (2011)
35. S. Giovanazzi, A. Gorlitz, and T. Pfau, Tuning the dipolar interaction in quantum gases, *Phys. Rev. Lett.* 89(13), 130401 (2002)
36. P. Pedri and L. Santos, Two-dimensional bright solitons in dipolar Bose–Einstein condensates, *Phys. Rev. Lett.* 95(20), 200404 (2005)
37. T. Koch, T. Lahaye, J. Metz, B. Frohlich, A. Griesmaier, and T. Pfau, Stabilization of a purely dipolar quantum gas against collapse, *Nat. Phys.* 4(3), 218 (2008)
38. I. Tikhonenkov, B. A. Malomed, and A. Vardi, Anisotropic solitons in dipolar Bose–Einstein condensates, *Phys. Rev. Lett.* 100(9), 090406 (2008)
39. Y. Li, J. Liu, W. Pang, and B. A. Malomed, Matter-wave solitons supported by field-induced dipole–dipole repulsion with spatially modulated strength, *Phys. Rev. A* 88(5), 053630 (2013).
40. Z. Luo, Y. Li, W. Pang, and Y. Liu, Dipolar matter-wave soliton in one-dimensional optical lattice with tunable local and nonlocal nonlinearities, *J. Phys. Soc. Jpn.* 82(9), 094401 (2013)
41. S. E. Pollack, D. Dries, M. Junker, Y. P. Chen, T. A. Corcovilos, and R. G. Hulet, Extreme tunability of interactions in a Li^7 Bose–Einstein condensate, *Phys. Rev. Lett.* 102(9), 090402 (2009)
42. L. P. Pitaevskii and A. Stringari, Bose–Einstein condensation, Clarendon Press, Oxford, 2003
43. Y. Li, J. Liu, W. Pang, and B. A. Malomed, Lattice solitons with quadrupolar intersite interactions, *Phys. Rev. A* 88(6), 063635 (2013)
44. L. D. Landau and E. M. Lifshitz, The Field Theory, Nauka-Publishers, Moscow, 1988
45. H. Sakaguchi and B. A. Malomed, Solitons in combined linear and nonlinear lattice potentials, *Phys. Rev. A* 81(1), 013624 (2010)
46. X. Zhang, J. Chai, J. Huang, Z. Chen, Y. Li, and B. A. Malomed, Discrete solitons and scattering of lattice waves in guiding arrays with a nonlinear $\mathcal{PT}$-symmetric defect, *Opt. Exp.* 22(11), 13927 (2014)
47. M. L. Chiofalo, S. Succi, and M. P. Tosi, Ground state of trapped interacting Bose–Einstein condensates by an explicit imaginary-time algorithm, *Phys. Rev. E* 62(5), 7438 (2000)
48. J. Yang and T. I. Lakoba, Accelerated imaginary-time evolution methods for the computation of solitary waves, *Stud. Appl. Math.* 120(3), 265 (2008)
49. J. Yang and T. I. Lakoba, Universally-convergent squared-operator iteration methods for solitary waves in general nonlinear wave equations, *Stud. Appl. Math.* 118(2), 153 (2007)
50. G. P. Agrawal, Nonlinear Fiber Optics, Academic Press, 2007
51. Z. Chen, J. Liu, S. Fu, Y. Li, and B. A. Malomed, Discrete solitons and vortices on two-dimensional lattices of $\mathcal{PT}$-symmetric couplers, *Opt. Exp.* 22(24), 029679 (2014)